Observation of Backaction and Self-Induced Trapping in a Planar Hollow Photonic Crystal Cavity

Nicolas Descharmes, Ulagalandha Perumal Dharanipathy, Zhaolu Diao, Mario Tonin, and Romuald Houdré
Institut de Physique de la Matière Condensée, École Polytechnique Fédérale de Lausanne (EPFL), Station 3, CH-1015 Lausanne, Switzerland
(Received 20 December 2012; published 20 March 2013)

The optomechanical coupling between a resonant optical field and a nanoparticle through trapping forces is demonstrated. Resonant optical trapping, when achieved in a hollow photonic crystal cavity is accompanied by cavity backaction effects that result from two mechanisms. First, the effect of the particle on the resonant field is measured as a shift in the cavity eigenfrequency. Second, the effect of the resonant field on the particle is shown as a wavelength-dependent trapping strength. The existence of two distinct trapping regimes, intrinsically particle specific, is also revealed. Long optical trapping (> 10 min) of 500 nm dielectric particles is achieved with very low intracavity powers (< 120 μW).

DOI: 10.1103/PhysRevLett.110.123601 PACS numbers: 42.50.Wk, 42.60.Da, 42.70.Qs, 87.80.Cc

Recent experiments have widely studied the coupling between a resonant optical field and single atoms [1,2] or micromechanical resonators [3,4]. However, the interaction between the mechanics of a large isolated nanoscale particle and a high finesse optical cavity, though theoretically predicted [5–8], is yet to be reported. Quantitative investigation of this optomechanical interaction requires the use of cavities with high quality factors (Q) and large field gradients. In this context, it has been suggested [6,9,10] that photonic crystal (PhC) cavities tailored with an appropriate mode configuration would qualify as excellent candidates. However, the inherent nature of light to concentrate in the high refractive index medium results in the fact that the trapped particle interacts only with a limited fraction of the optical field. As a first consequence, input laser powers required are in the order of tens or even hundreds of milliwatts. Nevertheless it has been predicted as early as 2006 that sub-mW trapping of 100 nm sized particles should be achievable [9]. The second consequence is that the cavity mode is weakly perturbed by the presence of a particle in its vicinity making standard PhC cavities unsuitable for noticeable backaction effects. To circumvent this issue, it is possible to design dielectric microcavities with a significant field overlap on the low index medium, which we will refer to as hollow optical cavities [11–13] in analogy with the hollow core fiber terminology. In such cavities, it is expected that the enhanced field overlap can simultaneously allow for quantification of the particle perturbation on the cavity mode and the observation of backaction [3,14] phenomena.

In this work, the backaction between a resonant field in a planar photonic crystal cavity and a single dielectric nanoparticle through optical gradient forces is clearly evidenced for the first time. This phenomenon, where the motion of the center of mass of the particle and the cavity field are mutually coupled, derives from two classical mechanisms. The first one is the existence of strong optical forces and is assessed by stably trapping the particle within the cavity over tens of minutes. The converse mechanism is a dynamic eigenmode perturbation and manifests as a large shift in the cavity resonance. The resulting coupling between the particle and the optical field is revealed in the wavelength-dependent trapping strength and confirms the existence of two distinct trapping regimes for the first time. In both the trapping regimes, the particle itself actively contributes to the evolution of the trapping forces constituting the first experimental demonstration of self-induced trapping [9].

In this experiment, the hollow structure consists of a circular defect (~ 700 nm in diameter) in a triangular PhC lattice on a silicon membrane [cf. Fig. 1(b)]. This cavity allows for a hexapole field distribution as shown in Fig. 1(a) displaying experimental quality factors of up to 2000 in water ($Q_{\mathrm{FEM}} \sim 3300$), an estimated mode volume of 0.36 μm^3 and field overlap of 15% with the volume enclosed by the circular defect. The hollow photonic crystal cavities are implemented in a 30×12 mm integrated optofluidic chip [15,16]. Resonant excitation of the photonic crystal cavities is performed using a tuneable laser diode coupled to lensed fibers in an end-fire setup. A two-layer, 170 μm-thick, polydimethylsiloxane membrane has been developed to bring the particle in the vicinity of the cavity while maintaining high numerical aperture imaging from the top. The microfluidic circuitry includes pressure driven valves [17] that enable us to control the flow precisely in the channel. The flow in the channel is arrested, placing the particles in nonconstrained Brownian motion near the cavity region.

It can be seen in Fig. 1(c) that the cavity field extends over a few hundred nanometres above and below the surface of the slab. This allows for the capturing of a particle in the vicinity of the circular defect. The field gradient along the vertical direction gives rise to a restoring force pulling the particle towards the central plane of

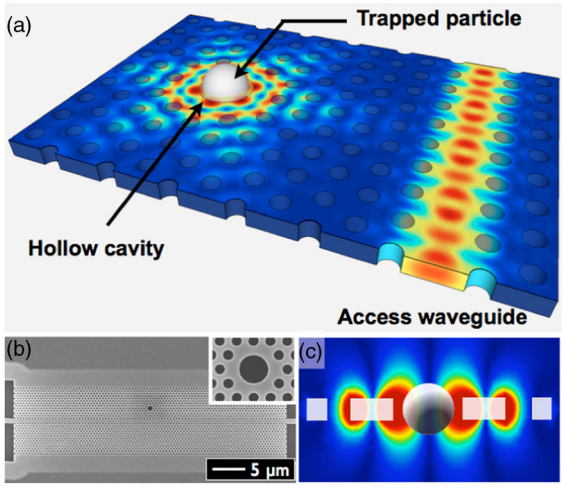

FIG. 1 (color online). Hollow photonic crystal cavity. (a) Computed electric field distribution in a hollow circular cavity in the presence of a 500 nm dielectric particle. (b) Scanning electron micrograph of the PhC device showing both the circular cavity and the coupling waveguide. Inset: 10 × magnification of the circular defect (700 nm in diameter). (c) Distribution of the electric field in a vertical cross section of the photonic crystal, centered on the particle, as computed with 3D finite elements (COMSOL).

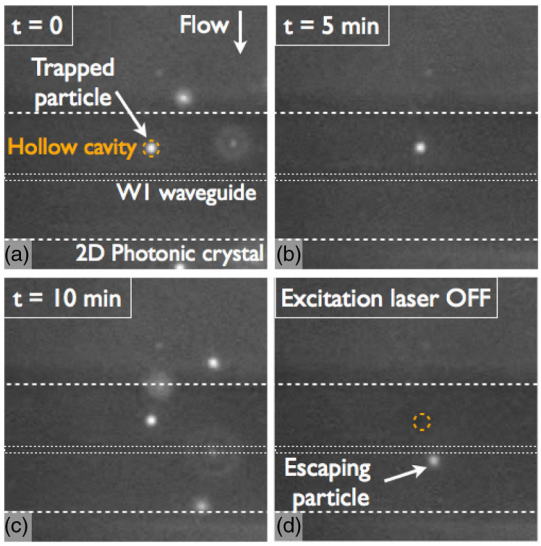

FIG. 2 (color online). Resonant optical trapping inside the hollow photonic crystal cavity. (a) A single 500 nm fluorescent particle is resonantly trapped inside the photonic crystal cavity region with a waveguide power lower than 120 μW. (b), (c) The particle remains strongly trapped for 10 min while other fluorescent particles are seen in the flow near the trapped particle. (d) The particle immediately leaves the cavity when the excitation laser is turned off after 10 min of continuous trapping.

the slab. The particle can be permanently trapped [18] [Fig. 2(a)–2(c)] and released on demand [Fig. 2(d)] by turning off the excitation laser. Records of trapping times over 20 min have been achieved without apparent photodamage or photobleaching of the particle. Estimated power in the waveguide near the cavity is lower than 120 μW for the case of the permanent trap [19]. Shorter trapping times (few tens of seconds) have been observed for guided powers as low as 37 μW. These unique trapping characteristics are the direct consequence of accessing the internal cavity field, in contrast to schemes [20,21] involving only the evanescent tail of a resonant mode.

As introduced before, the presence of the particle generates a local perturbation of the intracavity refractive index that results in a shift (δ) of the cavity resonance wavelength. It is possible to follow the evolution of this shift with time using two laser sources. The first laser excites the cavity eigenmode at a fixed wavelength, which traps the particle as explained before. The second laser, of weaker intensity, is coupled through the same end-fire setup using a 90/10 fiber coupler. In this manner, the cavity spectrum can be acquired without altering the characteristics of the resonant trap. The weak probe laser intensity is modulated so that it can be extracted from the stronger trapping laser signal with the use of a lock-in detection. The evolution of the spectrum in time with a scanning rate of 1 Hz is displayed in Fig. 3(a), which shows the optical response in the presence or absence of a particle within the cavity. The fluctuations of the cavity spectrum in the presence of the particle demonstrate the truly suspended feature of the trap and the constricted residual Brownian motion within the stable trap region. A snapshot [cf. Fig. 3(b)] shows an average resonance shift of 1.8 nm from the unloaded cavity resonance (λ_U). This shift is as large as twice the linewidth ($\Delta\lambda$) of the unperturbed cavity mode. The apparent linewidth broadening in the presence of a particle is attributed to an averaging effect of the slow acquisition time of the measurement setup. Theoretical computations were performed with a 3D finite element method solver (COMSOL) to observe the change in the eigenfrequency of the system as the particle is moved inside the cavity volume. The resonance wavelength shifts induced by particles of different diameters are computed and summarized in Fig. 3(c). The magnitude of the shifts primarily depends on the overlap integral of the cavity field on the volume of the particle. A maximum shift of 2.9 nm is obtained in the case of a 500 nm polystyrene particle and is in reasonable agreement with the measurements shown before. As the size of the particle is progressively decreased, the maximum computed shift scales down rapidly. In the case of polystyrene particles smaller than 100 nm, the extremely weak particle-cavity interaction will make the backaction effects vanish. Moreover, a deviation of the particle's position from the cavity center along the vertical axis strongly reduces the magnitude of the wavelength shift.

When the particle is in Brownian motion within the hollow volume of the cavity, both the trapping and shift

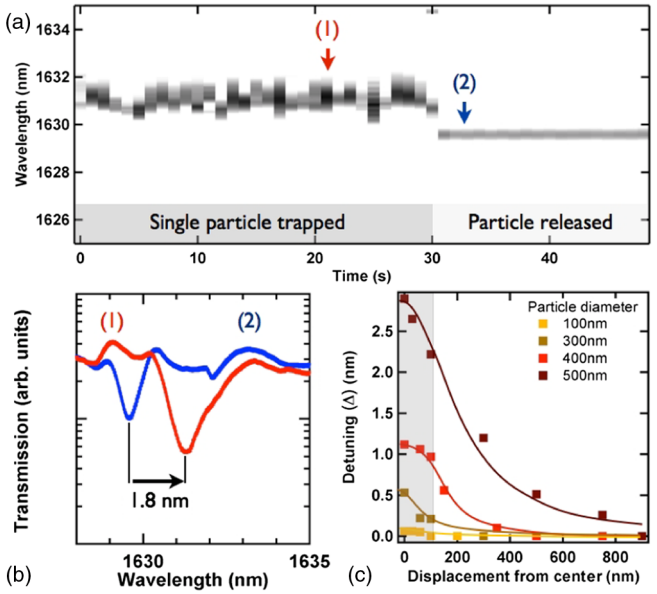

FIG. 3 (color online). Demonstration of particle-induced resonance frequency shift. (a) Record of the evolution of the cavity spectrum in time while a particle is trapped in the cavity and after it is released. (b) A single snapshot from (a), displaying an average resonance shift of 1.8 nm from the unloaded cavity resonance. (c) Computed resonance wavelength shifts as a function of particle size as it is moved along the vertical direction from the center of the cavity. The shaded area (in grey) shows the extent of the silicon slab. A maximum shift of 2.9 nm is found for a 500 nm particle placed in the center of the cavity.

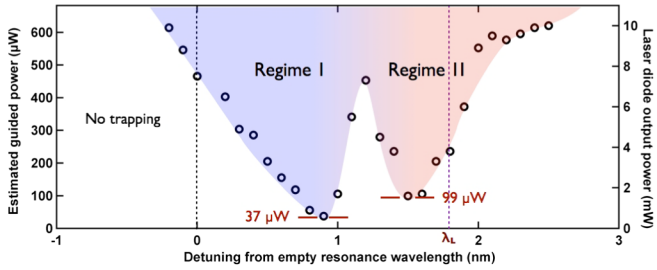

FIG. 4 (color online). Demonstration of particle-cavity coupling. Record of trapping threshold powers as a function of the estimated guided power in the access waveguide (left axis) and the laser diode output power (right axis). Experimental points correspond to escape trapping times of the order of 10 s.

phenomena described before occur in a coupled manner. This coupling is at the core of the particle-cavity backaction, wherein the trapping characteristics strongly depend on the excitation wavelength. The Brownian motion induces resonance wavelength shifts, which, for a monochromatic excitation, renormalizes the amount of energy coupled to the cavity and consequently the trapping forces. Concurrently, the energy required by the particle to escape the resonant trap depends on the excitation wavelength in a nontrivial manner. In other words, the wavelength-dependent escape energy profile does not reproduce the loaded cavity optical response as would be expected from a noncoupled system. On the contrary, a more complex profile extending over several cavity linewidths is observed. As a direct signature of the backaction effect, the largest escape energy required for the particle to leave the trap is expected to occur neither at the unloaded (λ_U) nor at the loaded (λ_L) resonance wavelengths but in a region in between. This is demonstrated by monitoring the trapping threshold power for a range of wavelengths centred on λ_U. While a particle is held in the resonant trap for a given wavelength, the excitation power is progressively decreased until the particle escapes. Figure 4 reports the evolution of the escape threshold power for a range of wavelengths detuned from λ_U. As expected, the resonant nature of the trap not only results in a restricted range of wavelengths only for which it is possible to observe trapping but also two distinct minima associated with two trapping regimes can be observed. The first regime (I) has a large trapping bandwidth and the lowest threshold power of 37 μW. The second regime (II) covers a narrower bandwidth centred near λ_L and has a larger threshold power of 99 μW.

The forces acting on the particle were computed by using the Maxwell's stress tensor formalism integrated over the surface of the spherical particle for various detuning values. The trapping forces for a 500 nm dielectric particle are presented in Fig. 5(a), taking into account the field renormalization effect. It can be seen that the magnitude of the out-of-plane and in-plane force components experienced by the particle vary with detuning. In the case of the out-of-plane component, the position of the maximum force is also a detuning-dependent quantity. In addition to this, the restoring force profile displays a large degree of anharmonicity. Finally, one can notice that the out-of-plane and in-plane components get sequentially predominant with detuning leading to the existence of the two experimentally observed regimes. The first regime can be conceptualized as a quasi-1D trap as illustrated in Fig. 5(b), where the particle is held within the hollow volume wherein it experiences weak trapping forces. As soon as the particle deviates from the cavity volume, the intracavity field builds up and strong pulling forces arise in the vertical direction bringing it back to the center of the trap. In these detuning values, the in-plane forces are considerably weaker compared to their out-of-plane counterparts. The second regime appears at the farther detuning values, closer to the loaded cavity wavelength. It can be seen as a 3D trap where the stable position is located near the inner sidewalls of the cavity as illustrated in Fig. 5(c). This position corresponds to the maximum field amplitude and hence the magnitudes of the forces are larger. For these detuning values, the in-plane force component is larger than the out-of-plane one. A maximum in-plane force of 1.5 nN is computed near the sidewall of the cavity for an

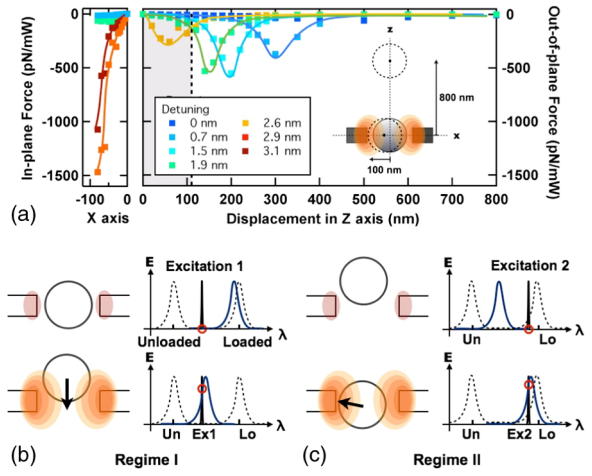

FIG. 5 (color online). (a) Theoretical computations for a 500 nm particle including the particle-cavity renormalization effect: Trapping forces as a function of the position of the particle for various detuning values along the horizontal axis inside the cavity (from −100 nm to 0) and along the vertical axis (0 to 800 nm). The shaded area corresponds to the half-thickness of the silicon slab. (b) Illustration of the first trapping regime. The eigenmode of the particle located in the cavity is weakly coupled to the excitation laser (λ_{Ex1}). An out-of-plane displacement of the particle couples the eigenmode back to the excitation resulting in strong gradient forces. (c) Illustration of the second trapping regime. A particle outside the cavity weakly couples the eigenmode to the excitation laser (λ_{Ex2}). As soon as the particle enters further into the cavity, the eigenmode is strongly coupled to the excitation and hence increases the trapping strength.

input power of 1 mW, which corresponds to a 3 orders of magnitude increase compared to previous studies involving evanescent field trapping [20].

In summary, self-induced trapping along with the back-action between a resonant optical field and a single nanoparticle has been reported. This mechanism opens the door to new kinds of all-optical schemes where single biological entities like cell organelles and viruses can be isolated, analyzed, and sorted depending on their size, shape, and optical properties. The novel trapping mechanisms can be extended to a variety of sizes owing to the scalability of photonic crystals. An additional remarkable fact from this scheme is that it addresses both the lack of exclusivity and specificity of standard optical tweezers [22]. The long trapping times along with very small residual Brownian motion is of major interest for studies that use spatially resolved spectroscopy. These results open the way to the exploration of such coupled systems where dynamical effects are expected to play a dramatic role [5].

We would like to thank Professor Sebastian Maerkl for his support in the fabrication of the microfluidic circuit. The authors acknowledge the financial support from the Swiss National Centre of Competence in Research Quantum Photonics and the Swiss National Science Foundation Projects No. 200021_134541 and 200020_140406.

[1] T. Aoki, B. Dayan, E. Wilcut, W. P. Bowen, A. S. Parkins, T. J. Kippenberg, K. J. Vahala, and H. J. Kimble, Nature (London) **443**, 671 (2006).
[2] J. McKeever, J. R. Buck, A. D. Boozer, A. Kuzmich, H. C. Nägerl, D. M. Stamper-Kurn, and H. J. Kimble, Phys. Rev. Lett. **90**, 133602 (2003).
[3] T. J. Kippenberg and K. J. Vahala, Science **321**, 1172 (2008).
[4] A. Naik, O. Buu, M. D. LaHaye, A. D. Armour, A. A. Clerk, M. P. Blencowe, and K. C. Schwab, Nature (London) **443**, 193 (2006).
[5] P. F. Barker and M. N. Shneider, Phys. Rev. A **81**, 023826 (2010).
[6] J. Hu, S. Lin, L. C. Kimerling, and K. Crozier, Phys. Rev. A **82**, 053819 (2010).
[7] D. E. Chang, C. A. Regal, S. B. Papp, D. J. Wilson, J. Ye, O. Painter, H. J. Kimble, and P. Zoller, Proc. Natl. Acad. Sci. U.S.A. **107**, 1005 (2010).
[8] O. Romero-Isart, A. C. Pflanzer, M. L. Juan, R. Quidant, N. Kiesel, M. Aspelmeyer, and J. I. Cirac, Phys. Rev. A **83**, 013803 (2011).
[9] M. Barth and O. Benson, Appl. Phys. Lett. **89**, 253114 (2006).
[10] A. Rahmani and P. C. Chaumet, Opt. Express **14**, 6353 (2006).
[11] M. R. Lee and P. M. Fauchet, Opt. Lett. **32**, 3284 (2007).
[12] A. Di Falco, L. O'Faolain, and T. F. Krauss, Appl. Phys. Lett. **94**, 063503 (2009).
[13] J. Jágerská, H. Zhang, Z. Diao, N. Le Thomas, and R. Houdré, Opt. Lett. **35**, 2523 (2010).
[14] M. L. Juan, R. Gordon, Y. Pang, F. Eftekhari, and R. Quidant, Nat. Phys. **5**, 915 (2009).
[15] D. Psaltis, S. R. Quake, and C. Yang, Nature (London) **442**, 381 (2006).
[16] C. Monat, P. Domachuk, and B. J. Eggleton, Nat. Photonics **1**, 106 (2007).
[17] M. A. Unger, H.-P. Chou, T. Thorsen, A. Scherer, and S. R. Quake, Science **288**, 113 (2000).
[18] See Supplemental Material at http://link.aps.org/supplemental/10.1103/PhysRevLett.110.123601 for movie with a detailed demonstration of positioning, trapping, and releasing of a 500 nm dielectric particle in a 2D photonic crystal hollow cavity.
[19] See Supplementary Material at http://link.aps.org/supplemental/10.1103/PhysRevLett.110.123601 for method and details on the estimation of guided power.
[20] S. Mandal, X. Serey, and D. Erickson, Nano Lett. **10**, 99 (2010).
[21] S. Lin, E. Schonbrun, and K. Crozier, Nano Lett. **10**, 2408 (2010).
[22] K. C. Neuman and A. Nagy, Nat. Methods **5**, 491 (2008).